Suppression of spin polarization in graphene nanoribbons by edge defects and impurities

Bing Huang,[1] Feng Liu,[2,*] Jian Wu,[1] Bing-Lin Gu,[1] and Wenhui Duan[1,†]

[1]*Department of Physics, Tsinghua University, Beijing 100084, People's Republic of China*
[2]*Department of Materials Science and Engineering, University of Utah, Salt Lake City, Utah 84112, USA*
(Received 31 March 2008; published 25 April 2008)

We investigate the effect of edge defects (vacancies) and impurities (substitutional dopants) on the robustness of spin polarization in graphene nanoribbons (GNRs) with zigzag edges by using density-functional-theory calculations. The stability of the spin state and its magnetic moments is found to continuously decrease with increasing the concentration of the defects or impurities. The system generally becomes nonmagnetic at the concentration of one edge defect (impurity) per ~10 Å. The spin suppression is shown to be caused by the reduction and removal of edge states at the Fermi energy. Our analysis implies an important criterion on the GNR samples for spintronics applications.

Graphene nanoribbons (GNRs) have attracted much recent interest because of their unique electronic properties and potential for device applications.[1–11] Of particular interest are those GNRs with zigzag edges, which are shown to have a spin-polarized ground state.[4,5,8] The spin polarization originated from the edge states that introduce a high density of state at the Fermi energy. It can be qualitatively understood in terms of the Stoner magnetism of *sp* electrons (in analogy to conventional *d* electrons) occupying a very narrow edge band to render instability of spin-band splitting.[12] The spins are found to be localized on the ribbon edges, with ferromagnetic coupling within each edge and antiferromagnetic coupling between the two edges.

Because the magnetism in GNRs resulted from the highly degenerate edge states, it must require a perfect edge structure. However, real samples of GNRs (Ref. 9) are unlikely to have perfect edges but contain structural defects and impurities of foreign atomic species. Thus, one important question is how robust the spin state is in the presence of edge defects and impurities. The answer to this question not only is scientifically interesting to better understand the physical mechanisms of spin polarization in GNRs but also has important technological implications if GNRs are to be realized as a new class of spintronic materials. Some existing studies[5] seemed to suggest that the spins in GNRs are robust against the formation of edge defects at certain concentrations. However, in this Brief Report, we show that the spins can be completely removed by edge defects or impurities at concentrations accessible in real samples, which renders a practical difficulty in realizing spin polarization in GNRs.

We have performed a systematic study of the stability and degree of spin polarization in GNRs as a function of the concentration of edge defects and impurities by using first-principles density-functional-theory (DFT) calculations. We chose vacancy and substitutional boron (B) atom as typical examples of a structural edge defect and impurity, respectively, since vacancies are expected to be the most abundant defects in a roughened edge and B atoms are a common choice of electronic dopants.[7,6] Our calculations show that the spin is completely suppressed at the defect (impurity) sites, while it may preserve on those sites away from defects (impurities) when the defect (impurity) concentration is low. The stability of the spin state and its "average" magnetic

moment continuously decreases with increasing the defect (impurity) concentration. Typically, independent of the ribbon width, the system becomes nonmagnetic at the critical concentration of one edge defect (impurity) per ~10 Å, which is a concentration shown to be accessible in real samples based on thermodynamic considerations. The magnetism can also be locally "dead" in between two defects (impurities) as long as they are closer than the third nearest-neighbor (NN) positions. The spin suppression closely correlates with the reduction and removal of edge states at the Fermi energy.

Our calculations are performed using the DFT pseudopotential plane-wave method within the local spin-density approximation.[13] The plane-wave cut-off energy is set as 450 eV. The structure optimization has been performed until the residual atomic forces are less than 0.01 eV/Å. We calculated GNRs with H-terminated zigzag edges with two different widths, namely, the (2.5,2.5) and (1.5,1.5) "armchair" ribbons,[7] by using a nomenclature in analogy to armchair carbon nanotubes that would unfold into corresponding ribbons with zigzag edges. Vacancies or impurities are introduced into the edge by removing edge C-H pairs or replacing C with B, respectively. Their concentrations are varied from 0.034 to 0.136 Å^{-1} along the edge, and both uniform and nonuniform distributions of defects (impurities) are considered.

Figure 1(a) shows the calculated ground-state spin distributions of a (2.5,2.5) GNR at an edge vacancy concentration of 0.034 Å^{-1}. The spin polarization is mostly localized on the edges with the top and bottom edge spins antiferromagnetic coupled with each other. One notices that spin is locally absent at the vacancy sites and it increases as one moves away from the vacancy along the edge. Figure 1(b) shows the ground-state spin distributions at a higher vacancy concentration of 0.068 Å^{-1}. Overall, the spins exhibit an identical distribution pattern, but their magnitude is reduced in comparison to those in Fig. 1(a). At an even higher vacancy concentration of 0.136 Å^{-1}, Fig. 1(c) shows that the spins are completely suppressed at all the atomic sites and the GNR becomes nonmagnetic. Almost identical results are obtained for B impurities, as shown in Figs. 1(d)–1(f).

In Fig. 1(g), we plot the magnetic moments on the top edge as a function of edge positions at four different vacancy
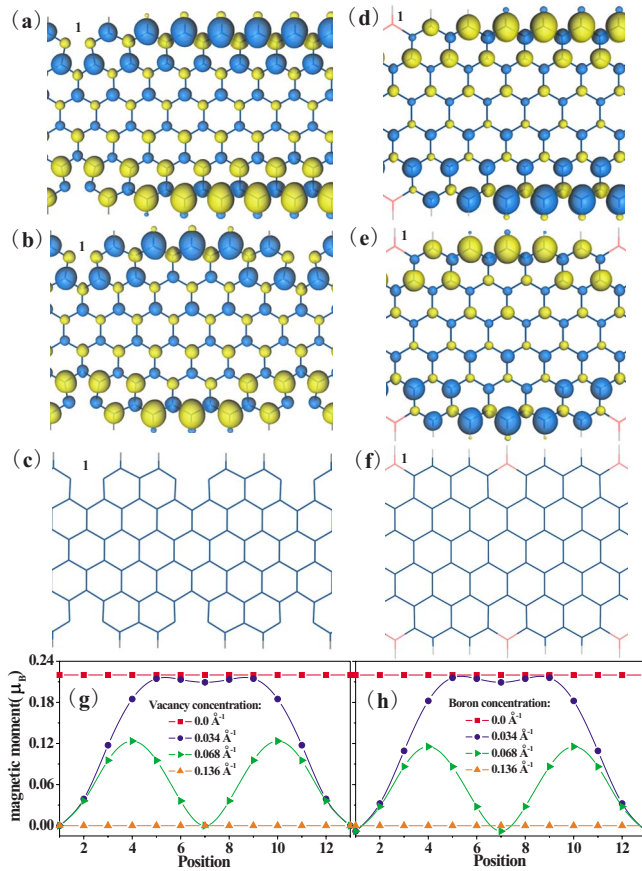
FIG. 1. (Color online) Isovalue surfaces of the charge difference between the spin-up and spin-down states of the ground states calculated for the (2.5,2.5) GNR at three different linear vacancy concentrations on the edge: (a) 0.034 Å^{-1}, (b) 0.068 Å^{-1}, and (c) 0.136 Å^{-1}. Half of the supercell in Fig. 1(a), one in Fig. 1(b), and two in Fig. 1(c) are shown. The yellow and blue surface represents the spin-up and spin-down states, respectively. The range of isovalues is set at $[-0.005:0.005]\mu_B \text{ Å}^{-1}$ in case (a) and $[-0.003:0.003]\mu_B \text{ Å}^{-1}$ in cases (b) and (c). [(d)–(f)] The same as (a)–(c) for B impurities. (g) The magnetic moment per edge atom on the top edge at three vacancy concentrations corresponding to cases (a)–(c), plus the case without vacancy. (h) The same as (g) for B impurities.

concentrations. Without vacancy, there is a uniform spin distribution with a large moment of $0.22\mu_B$ at every edge sites (red squares). When vacancies are introduced at a low enough concentration so that spins are preserved on the edges, the presence of vacancies in effect enforces a spin-density wave (oscillation) along the ribbon edge, with the zero moment (nodal point) at the vacancy site and the maximum moment in the middle between the vacancies (blue dots and green right triangles). The period of the spin-density wave equals the inverse of the vacancy concentration, while its amplitude decreases with increasing the concentration. At a sufficiently high concentration, the vacancies suppress all the spins and the moments become zero everywhere (orange up triangle). The same results are obtained for B impurities, as shown in Fig. 1(h).

The results in Fig. 1 indicate that the spin polarization decreases with increasing the edge defect (impurity) concen-
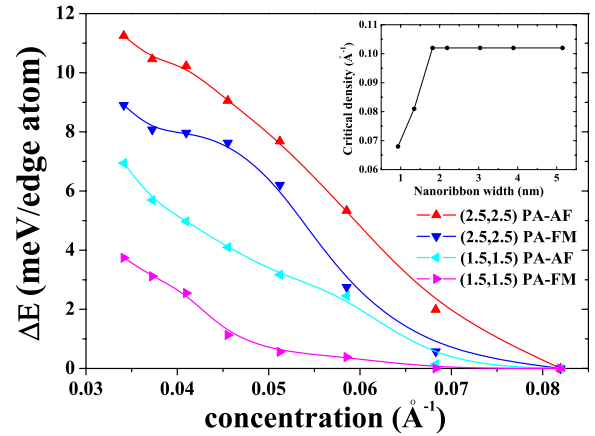
FIG. 2. (Color online) The energy difference per edge atom between the magnetic (AF or FM) and paramagnetic (PA) state as a function of vacancy concentration in the edge. Two different ribbon widths of (2.5, 2.5) and (1.5,1.5) are shown. The inset shows the critical concentration as a function of the ribbon width up to 5 nm.

tration and eventually vanishes. To further demonstrate this phenomenon, we have compared the relative stability of the spin state with that of the nonspin state. Figure 2 shows the calculated energy difference per edge atom as a function of vacancy concentration. The results of B impurities are essentially the same. In general, the energy difference between the magnetic state [both antiferromagnetic (AF) and ferromagnetic (FM)] and the nonmagnetic state rapidly decreases with increasing the defect (impurity) concentration. Eventually, the difference decreases to zero and the GNR becomes nonmagnetic. We have examined the critical defect (impurity) concentration at which the spin vanishes as a function of the ribbon width from 1 to 5 nm, as shown in the inset of Fig. 2 (note that the curve is discontinuous at the point of 2 nm because we can only discretely change the ribbon width and concentration). We found that the spin polarization is completely suppressed at a typical critical defect (impurity) concentration of ~ 0.10 Å^{-1} when the ribbon width is larger than 2 nm. The critical concentration is lower in narrower ribbons, e.g., at 0.081 Å^{-1} for a (2.5,2.5) ribbon and at 0.068 Å^{-1} for a (1.5,1.5) ribbon.

Given the critical concentration of 0.10 Å^{-1}, the next important question is whether such a concentration is accessible in real samples. Thus, we have calculated the formation energies of edge defects and impurities. For vacancy formation, we obtain $\Delta E = 9.21$ eV$+\mu_C$ for removing a C away from the edge, where μ_C is the chemical potential of C, which may vary from -10.13 eV (bulk graphene) to -1.25 eV (atomic C). Now, if we consider the vacancy to be thermally activated, then at room temperature, the critical concentration of 0.10 Å^{-1} can be achieved by a formation energy of 0.035 eV. This requires a C chemical potential of -9.175 eV, which is within the possible range of C chemical potential variation. In addition to thermal excitation, vacancies or structural defects are also created by a nanopatterning process. In fact, presently, the ribbons can only be made with very rough edges containing a high concentration of defects.[9] Thus, the critical density we identify here is likely to be accessible in real samples. This will likely pose a practical
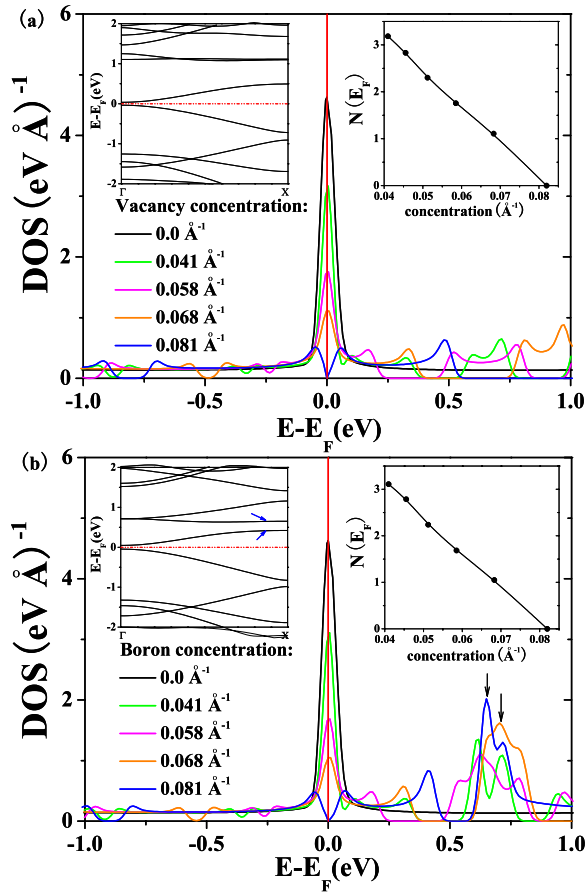
FIG. 3. (Color online) (a)The calculated total DOS for a (2.5,2.5) ribbon in the paramagnetic state at five different vacancy edge concentration. Up-left inset: the band structure at the vacancy concentration of 0.081 Å^{-1}. Up-right inset: the DOS at E_F as a function of vacancy concentration. (b) The same as (a) for B impurities.

challenge in realizing the spin polarization in GNRs. For the case of B impurity, we obtain $\Delta E = 2.49$ eV $+ \mu_C - \mu_B$, where the chemical potential of B may vary from -7.49 eV (α phase B) to -0.31 eV (atomic B). In this case, the critical concentration of B is accessible by increasing the B partial pressure and, hence, its chemical potential in the doping process.

The magnetism resulted from a high density of state (DOS) at the Fermi energy (E_F) that renders instability of spin polarization. Consequently, one expects that the suppression of magnetism is correlated with the change in DOS at E_F induced by defects (impurities). We have examined the DOS as a function of defect (impurity) concentration, which has indeed confirmed such mechanism. In Fig. 3(a), we plot the DOS in the paramagnetic state of the (2.5,2.5) ribbon as a function of vacancy concentration. Clearly, the DOS at E_F decreases almost linearly (up-right inset) with increasing the vacancy concentration, which is in close correlation with the magnetization shown in Figs. 1 and 2. As the defect concentration reaches 0.081 Å^{-1}, the DOS at E_F falls to zero, and the system becomes nonmagnetic. Without defects, the highly degenerate edge states in a perfect ribbon edge give rise to the high DOS at E_F. Since the vacancies will not

contribute to the same edge state, their presence decreases the DOS at E_F.

Similarly, in Fig. 3(b), we plot the DOS in the paramagnetic state of the (2.5,2.5) ribbon as a function of B impurity concentration. Again, the DOS at E_F decreases almost linearly (up-right inset) with increasing the B concentration and eventually vanishes, so that the ribbon becomes nonmagnetic. However, here, the mechanism of DOS reduction at E_F is slightly different from that in the case of vacancy. The impurity B atoms act as electronic dopants to introduce impurity states (levels) away from the Fermi energy, so as to reduce the DOS at E_F. This can be seen in Fig. 3(b) when the DOS at E_F decreases and vanishes at $E=0$ with increasing the B concentration, another peak of DOS appears and increases at $E=0.7$ eV. Those bands of edge states (up-left inset) being shifted to 0.7 eV are indicated by arrows. So, effectively, the B impurities lift the degeneracy of the edge states and, hence, decrease the DOS at E_F. In addition, the corresponding band structure (up-left inset) shows the system becoming semiconducting with a small band gap upon B doping. (We have also studied the case of N atoms, which showed the same effect as B atoms except that the impurity edge states were shifted to below Fermi energy since N is a n-type dopant.)

We may further understand the spin suppression by edge defect (impurity) in the context of itinerant ferromagnetism and local order.[14–16] It has been shown that the magnetic moment in an itinerant magnetic material strongly depends on the local coordination.[14,15] When a nonmagnetic "impurity" is introduced in the magnetic medium, the moment is greatly suppressed at the impurity site and its vicinity.[15] Conversely, when a magnetic element is introduced in a nonmagnetic medium, its moment is quenched at low concentrations but can be redeveloped at high concentrations and there is a strong correlation between the magnetic dopants.[16]

Similarly, our case here can be thought of as doping the magnetic medium of itinerant sp electrons[12] with nonmagnetic impurities, vacancy, or B atom, which will suppress the magnetic moment at the impurity site and its vicinity. When two and more impurities are introduced, the correlation between them would determine the local state of moment (spin polarization). To test this idea, we have examined the local magnetic moment in between two defects (or impurities) as a function of their separation. From Figs. 4(a)–4(c), we see that the local moment in between the two vacancies decreases as the two vacancies move closer and completely vanishes when they are at the third NN position [Fig. 4(c)]. The same result is also obtained at even lower defect concentrations. This means that spin suppression is a rather localized effect. For example, we can selectively introduce defects (impurities) in only one ribbon edge while keeping the other edge perfect. Then, we will create a ferromagnetic order along one ribbon edge while the other edge is nonmagnetic, as shown in Fig. 5, which could be useful for spintronics applications if ferromagnetism is desired.

In conclusion, we have examined the robustness of spin polarization in GNRs with zigzag edge by using first-principles calculations. We show that the spin polarization can be greatly suppressed in the presence of edge defects and impurities. In general, the GNR becomes nonmagnetic at a
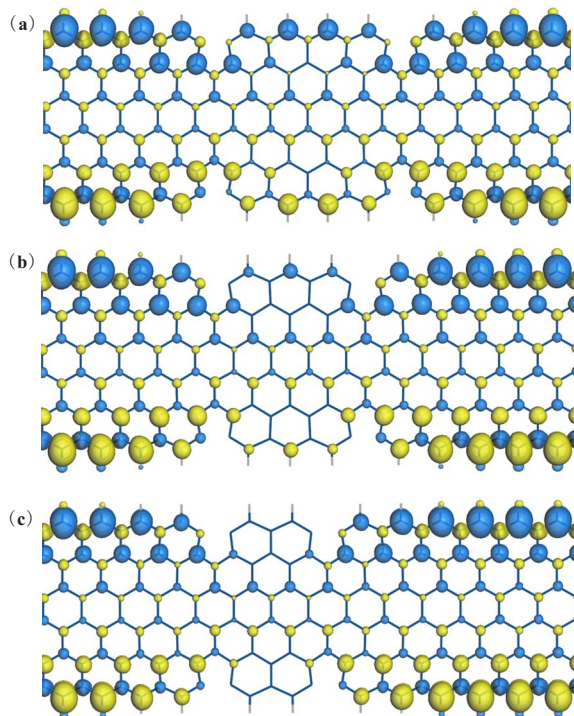
FIG. 4. (Color online) Similar to Fig. 1(a) but with the vacancies moving closer from (a) the fifth NN position (even distribution) to (b) the fourth NN position and to (c) the third NN position. The range of isovalues is set at $[-0.004:0.004]\mu_B \text{ Å}^{-1}$.

critical edge defect (impurity) concentration of $\sim$0.10 Å^{-1}, which is shown to be accessible in real samples. The magnetic moments may also locally vanish if two defects (impurities) randomly occur to be closer than the third NN distance. The spin suppression closely correlates with the
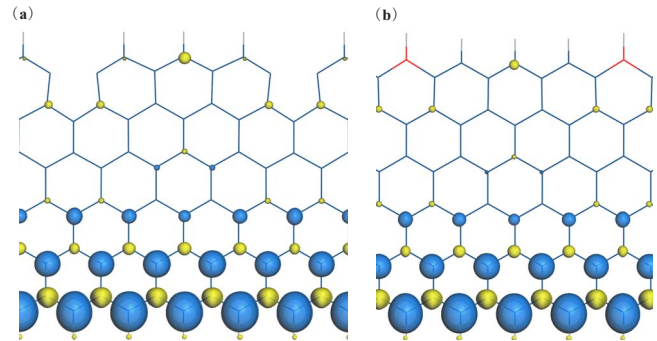
FIG. 5. (Color online) Similar to Fig. 1(a) but with (a) vacancy and (b) B impurity introduced at only one of the two ribbon edges at the fourth NN positions. The range of isovalues is set at $[-0.005:0.005]\mu_B \text{ Å}^{-1}$.

reduction of DOS at the Fermi energy induced by defects (impurities). It can be qualitatively understood in the context of itinerant magnetism and local order. Our findings indicate that although the magnetic properties of GNRs are of great scientific interest, practical realization of spin polarization in GNRs for spintronics applications can be rather challenging. On the one hand, the overall spin state can be completely removed by a high defect (impurity) concentration and, on the other hand, the local spins can be suppressed by small randomness of the edge structure with a few concentrated defects, which can be detrimental to "one-dimensional" spin transport along the edge.

*fliu@eng.utah.edu

†dwh@phys.tsinguha.edu.cn

[1] K. Nakada, M. Fujita, G. Dresselhaus, and M. S. Dresselhaus, Phys. Rev. B **54**, 17954 (1996).

[2] K. Wakabayashi, M. Fujita, H. Ajiki, and M. Sigrist, Phys. Rev. B **59**, 8271 (1999).

[3] K. Kusakabe and M. Maruyama, Phys. Rev. B **67**, 092406 (2003).

[4] H. Lee, Y.-W. Son, N. Park, S. Han, and J. Yu, Phys. Rev. B **72**, 174431 (2005).

[5] Y.-W. Son, M. L. Cohen, and S. G. Louie, Nature (London) **444**, 347 (2006); Phys. Rev. Lett. **97**, 216803 (2006).

[6] T. B. Martins, R. H. Miwa, A. J. R. da Silva, and A. Fazzio, Phys. Rev. Lett. **98**, 196803 (2007).

[7] Q. M. Yan, B. Huang, J. Yu, F. W. Zheng, J. Zang, J. Wu, B. L. Gu, F. Liu, and W. H. Duan, Nano Lett. **7**, 1469 (2007).

[8] L. Pisani, J. A. Chan, B. Montanari, and N. M. Harrison, Phys. Rev. B **75**, 064418 (2007).

[9] M. Y. Han, B. Ozyilmaz, Y. Zhang, and P. Kim, Phys. Rev. Lett. **98**, 206805 (2007).

[10] O. Hod, V. Barone, J. E. Peralta, and G. E. Scuseria, Nano Lett. **7**, 2295 (2007).

[11] D. Gunlyckea, D. A. Areshkin, and C. T. White, Appl. Phys. Lett. **90**, 142104 (2007).

[12] D. M. Edwards and M. I. Katsnelson, J. Phys.: Condens. Matter **18**, 7209 (2006).

[13] G. Kresse and J. Furthmüller, Comput. Mater. Sci. **6**, 15 (1996).

[14] F. Liu, M. R. Press, S. N. Khanna, and P. Jena, Phys. Rev. B **39**, 6914 (1989).

[15] M. R. Press, F. Liu, S. N. Khanna, and P. Jena, Phys. Rev. B **40**, 399 (1989).

[16] F. Liu, S. N. Khanna, L. Magaud, P. Jena, V. de Coulon, F. Reuse, S. S. Jaswal, X.-G. He, and F. Cyrot-Lackman, Phys. Rev. B **48**, 1295 (1993).